

Salvianolic acid B reverses multidrug resistance in nude mice bearing human colon cancer stem cells

PIAOTING GUO¹, JIANCHAO WANG², WENCANG GAO³, XIA LIU²,
SHAOFEI WU⁴, BOSHUN WAN⁵, LEI XU⁶ and YANHUA LI¹

Departments of ¹General Medicine, ²Center Laboratory and ³Medical Oncology, The Second Affiliated Hospital of Zhejiang Chinese Medical University, Hangzhou, Zhejiang 310005; ⁴Department of Hepatopathy, Shandong Provincial Qianfoshan Hospital, Jinan, Shandong 250014; ⁵Department of General Surgery, Jiading District Central Hospital Affiliated Shanghai University of Medical and Health Sciences, Shanghai 201899; ⁶Department of Gastroenterology, The Second Affiliated Hospital of Zhejiang Chinese Medical University, Hangzhou, Zhejiang 310005, P.R. China

Received September 15, 2017; Accepted April 9, 2018

DOI: 10.3892/mmr.2018.9086

Abstract. Salvianolic acid B (SalB) is a water-soluble phenolic compound, extractable from *Salvia miltiorrhiza*, and has previously been demonstrated to reverse tumor multidrug resistance (MDR) in colon cancer cells. Cancer stem cells (CSCs) are closely associated with drug resistance. Therefore, establishing a nude mouse model bearing human colon CSCs is important for the study of the mechanisms underlying colon cancer drug resistance as well as the reversal of drug resistance. The present study aimed to establish a nude mouse model bearing human colon CSCs and to investigate the effects of SalB on the drug resistance exhibited by the nude mouse model as well as determine its underlying mechanism. Cells from two colon cancer cell lines (LoVo and HCT-116) were cultured in serum-free medium to obtain CSCs-enriched spheroid cells. Following this, nude mice were transplanted with LoVo and HCT-116 colon CSCs to establish the CSC nude mouse model, which was subsequently demonstrated to exhibit MDR. The results of the present study revealed that following treatment with SalB, the chemotherapeutic drug resistance of xenografts was reversed to a certain extent. Western blot analysis was performed to investigate the expression levels of cluster of differentiation (CD)44, CD133, transcription factor sox-2 (SOX2) and ATP-binding cassette sub-family G member 2 (ABCG2) proteins, and the results demonstrated that treatment with SalB downregulated the expression of

CD44, SOX2 and ABCG2 proteins in both LoVo and HCT-116 colon CSCs xenografts. In conclusion, the results of the present study revealed that a serum-free suspension method can be performed to successfully isolate colon CSCs. In addition, a nude mice bearing colon CSCs animal model was successfully established, and associated tumors were confirmed to exhibit MDR. Furthermore, SalB was demonstrated to successfully reverse MDR in nude mice bearing LoVo and HCT-116 colon CSCs, as well as suppress the expression of CD44, SOX2 and ABCG2 proteins.

Introduction

Cancer multidrug resistance (MDR) is a major factor affecting chemotherapy efficacy, which may ultimately lead to the failure of chemotherapy (1). Cancer stem cells (CSCs) represent a cancer cell population with stem cell-like properties. Following the development of the cancer stem cell hypothesis as well as increasing research of stem cells in the oncology field, numerous studies have demonstrated that drug resistance exhibited by CSCs is an important factor affecting cancer MDR (2,3). Therapy targeting CSCs provides a novel therapeutic approach for clinical cancer therapy (4). Therefore, establishing an adaptable and feasible animal xenograft model bearing human colon CSCs is essential for the study of the underlying mechanisms of CSCs in order to develop novel and effective anticancer drugs.

At present, there is no agreement regarding the best method to acquire colon CSCs for the establishment of an animal model. There are three main methods routinely performed for the isolation and identification of colon CSCs. Firstly, specific expression of surface markers for CSCs can be determined, predominantly by flow cytometry (FCM) (5) and immunomagnetic beads sorting (6). In this method, isolation and identification are performed using expressed cell surface markers present on colon CSCs, including cluster of differentiation (CD)44, CD166, CD133, Nanog and transcription factor sox-2 (SOX2). This method has been widely used to identify and define CSCs. Secondly, Hoechst

Correspondence to: Dr Yanhua Li, Department of General Medicine, The Second Affiliated Hospital of Zhejiang Chinese Medical University, 318 Chaowang Road, Hangzhou, Zhejiang 310005, P.R. China
E-mail: 522135842@qq.com

Key words: salvianolic acid B, colon cancer stem cells, xenograft nude mice, drug resistance, stem cell markers

33342 staining can be performed to identify a population of cells with high ATP-binding cassette sub-family G member 2 (ABCG2) expression in colon cancer, as CSCs exhibiting enhanced ABCG2 expression can promote Hoechst 33342 efflux and decrease fluorescence intensity of intracellular DNA dye Hoechst 33342 (7). Lastly, a culture screening method based on the unique microenvironment required for the growth of colon CSCs can be performed to isolate and identify colon CSCs, of which serum-free suspension culture is the major method. CSCs can be isolated by creating an environment conducive for self-renewal and differentiation, as well as selective elimination of non-CSC cancer cells. This method has been widely applied for enriching CSCs (8). A nude mouse model for colon cancer can be established via subcutaneous injection or transplantation of xenograft tumor tissues (9,10); however, the methods required for the establishment of a CSC mouse model require further investigation.

Salvianolic acid B (SalB) is a water-soluble phenolic compound and is extractable from *Salvia miltiorrhiza* (11). SalB has previously been demonstrated to reduce the toxicity and enhance the efficacy of radiochemotherapy for the treatment of colon cancer, and its role in reversing tumor MDR has generated increasing attention (12,13). Stem cell factors, including SOX2, CD24, organic cation/carnitine transporter 4 (OCT4), CD29, CD44 and ABCG2; serve an important role in maintaining the morphology and function of colon CSCs, and are closely associated with the proliferation, drug resistance, invasion and migration of colon cancer cells (14-17). Investigation into the regulatory effects of SalB on CSC marker expression will further the understanding of the mechanisms underlying the effect of SalB on MDR reversal.

Two colon cancer cell lines (LoVo and HCT-116) were used in the present study to investigate the effect and underlying mechanism of SalB. The present study aimed to isolate and identify colon CSCs, establish a nude xenograft mouse model bearing colon CSCs, perform H&E staining, investigate the MDR of the xenografts and determine the efficacy of chemotherapy drugs on the mouse model. Furthermore, the present study aimed to investigate the effect of SalB on drug resistance exhibited by xenografts, determine the expression levels of CD44, CD133, SOX2 and ABCG2 following treatment with SalB, and investigate the underlying mechanism of this effect.

Materials and methods

Cell lines. Human colon cancer cell lines LoVo and HCT-116 were purchased from the Cell Resource Center, Shanghai Institutes for Biological Science (Shanghai, China).

Animals. A total of 100 specific pathogen free (SPF) BALB/c male nude mice were purchased from Shanghai SLAC Laboratory Animal Co., Ltd. [Shanghai, China; license no. SCXK (Hu) 2007-005]. Mice were aged 4 weeks and had a body weight of 18±2 g. All animal experiments were performed according to the guidelines of the Chinese Experimental Animals Administration Legislation and were approved by the Ethics Committee for Animal Experiments of Shanghai University of Traditional Chinese Medicine (Shanghai, China; reference no. SZY 201504023). Mice were fed in separate cages under specific pathogen-free conditions in a laminar flow chamber in the Lab

Animal Center, Shanghai University of Traditional Chinese Medicine (Shanghai, China). Standard water in drinking bottles and pelleted food were freely available to the mice. The temperature was maintained at 18-25°C at a relative humidity of 40-60% and a 12/12 h light/dark cycle. The cages, padding, feed and water were autoclaved at 121°C for 30 min. The padding was replaced at least twice a week. Animals were acclimatized for 1 week prior to the initiation of the experiments.

Drugs and reagents. SalB was purchased from Shanghai Winherb Medical Technology Co., Ltd. (Shanghai, China). A total of 100 mg of oxaliplatin (L-OHP) was purchased from Jiangsu Hengrui Medicine Co., Ltd. (Lianyungang, China; cat. no. H20040817). 5-Fluorouracil (5-FU) was purchased from Shanghai Xudong Haipu Pharmaceutical Co., Ltd. (Shanghai, China; 25 g/l; cat. no. 20070802). PRMI-1640 and DMEM/F12 were purchased from Hyclone; Thermo Fisher Scientific, Inc. (Waltham, MA, USA). Penicillin (5,000 IU/ml) and streptomycin (5,000 µg/ml) were purchased from Invitrogen; Thermo Fisher Scientific, Inc. (Waltham, MA, USA). Fetal bovine serum (FBS), L-glutamine, β-mercaptoethanol and 2-hydroxyethyl methacrylate were purchased from Sigma-Aldrich; Merck KGaA (Darmstadt, Germany). Recombinant human basic fibroblast growth factor, recombinant human epidermal growth factor, KnockOut Serum Replacement and 1% Non Essential Amino Acid (NEAA) were purchased from Gibco; Thermo Fisher Scientific, Inc. (Waltham, MA, USA). FcR Blocking Reagent was purchased from Miltenyi Biotec GmbH (Bergisch Gladbach, Germany). Anti-human CD133-PE and Mouse IgG2b kappa isotype control were purchased from eBioscience; Thermo Fisher Scientific, Inc.. A bicinchoninic acid assay (BCA) kit, Hematoxylin and Eosin Staining kit and an immunohistochemistry kit were purchased from Shanghai Beyotime Biological Science & Technology Co., Ltd. (Shanghai, China). Mouse monoclonal antibody ABCG2, mouse monoclonal antibody CD24, rabbit monoclonal antibody CD133, rabbit monoclonal antibody OCT-4, rabbit monoclonal antibody CD44, goat anti-mouse immunoglobulin G (IgG) and goat anti-rabbit IgG were all purchased from Abcam (Cambridge, MA, USA). Rabbit monoclonal antibody SOX2 was purchased from Cell Signaling Technology, Inc. (Danvers, MA, USA). RNA reverse kit and RNA amplification kit were purchased from Takara Bio, Inc. (Otsu, Japan).

Cell culture and spheroid formation. LoVo and HCT-116 cells were separately cultured in F-12K and McCoy5A medium, respectively. Both cultures contained 10% FBS, 100 µg/ml penicillin and 100 µg/ml streptomycin at 37°C, in a humidified 5% CO₂ incubator. Tumor cell spheres were isolated using the serum-free suspension culture method: Logarithmic growth phase LoVo and HCT-116 cells were trypsinized and centrifuged at 300 x g for 5 min at room temperature. The supernatant was then discarded and the precipitate was re-suspended with serum-free medium [Dulbecco's Modified Eagle Medium (DMEM)/F12 + KnockOut Serum Replacement (10-20%) + 1% NEAA + 1% L-glutamine + 0.1 mM β-mercaptoethanol + 20 µg/l recombinant human basic fibroblast growth factor + 20 µg/l recombinant human epidermal growth factor] and the cell resuspension was then added to a petridish coated with 2-hydroxyethyl methacrylate in a

Table I. DNA primer sequences.

Primer name	Sequence (5'→3')	
	Forward	Reverse
CD24	CCAGGGCAATGATGAATGAGA	GGGAGGCTGAGGCACGAGAAT
CD44	GGATGGACAAGTTTTGGTGGCAGC	GGTTACACCCCAATCTTCATGTCC
CD90	GACTGCCGCCATGAGAATAACACC	CGCGCCCGAGACTTGAA
CD133	GATTCATACTGGTGGCTGGGTGG	GCAGGTGAAGAGTGCCGTAAGT
SOX2	TTCGATCCCAACTTTCCAT	ACATCGATTCTCGGCAGAC
ABCG2	GGTTTCCAAGCGTTCATTCAA	TAGCCCAAAGTAAATGGCACCTA
OCT4	CGAAGAGAAAGCGAACCAGTATC	AGAACCACACTGGACCACATC
Nanog	GCAAAAAAGGAAGACAAGGTCC	CCTTCTGCGTCAACCATTG
GAPDH	GGTGGTCTCCTCTGACTTCAACA	CCAAATTCGTTGTCATACCAGGAAATG

CD, cluster of differentiation; SOX2, transcription factor Sox2; ABCG2, ATP binding cassette subfamily G member 2; OCT4, organic cation/carnitine transporter 4.

drop-wise manner (8). Cells were incubated at 37°C in 5% CO₂. Following 5-6 days of incubation, suspended CSCs spheroids were visible under a light microscope (magnification, x200).

Identification of colon CSCs. FCM was performed to determine CD133-positive expression. A single cell suspension (100 µl) containing 10⁶ cells/ml was prepared and treated with mouse IgG2b kappa FcR blocking reagent in an ice bath for 10 min and then incubated in the dark at 4°C for 30 min with phycoerythrin tagged CD133 (1:100; cat. no. 12-1339-41; eBioscience; Thermo Fisher Scientific, Inc.) and mouse IgG2b kappa isotype control (1:100; cat. no. 12-4732-81; eBioscience; Thermo Fisher Scientific, Inc.). Subsequently, the cells were washed twice with PBS and centrifuged at 300 x g for 10 min at 4°C. The supernatant was aspirated and 500 µl PBS (cat. no. C0221A; Shanghai Beyotime Biological Science & Technology Co., Ltd.) was added for analysis of the cells using a FACSCalibur (BD Biosciences, Franklin Lakes, NJ, USA).

Reverse transcription-quantitative polymerase chain reaction (RT-qPCR). RT-qPCR was performed to investigate the expression levels of CD90, CD24, CD44, CD133, SOX2, ABCG2, OCT4 and Nanog. Following the culture of adherent LoVo and HCT-116 cells in serum-free suspension media for ~5-6 days, suspended regular stem cell spheroids were visible, and spheroid cell suspension and adherent cells were simultaneously collected. Following this, total RNA was extracted using the RNeasy extraction kit (cat. no. 9108Q; Takara Biotechnology Co., Ltd., Dalian, China). Total RNA (1 µg) was subjected to RT at 42°C for 15 min followed by 95°C for 3 min using a FastQuant RT Kit (cat. no. KR106; Tiangen, Biotech Co., Ltd., Beijing, China). qPCR was performed using SYBR Green PCR Master Mix (cat. no. FP302; Tiangen, Biotech Co., Ltd.) in a ABI 7000 PCR instrument (Eppendorf, Hamburg, Germany) under the following thermocycling conditions: Initial denaturation at 95°C for 2 min; followed by 40 cycles of 95°C at 10 sec and 60°C at 30 sec. The threshold cycle (Cq) values of each sample were calculated using the 2^{-ΔΔCq} method (18). GAPDH was used as an internal control for the normalization of mRNA expression.

Experiments were performed in triplicate. Primer sequences for the targeting of the selected genes are presented in Table I.

Western blot analysis. Western blot analysis was performed to determine the expression levels of OCT4, CD24, CD44, CD133, SOX2 and ABCG2 proteins. Cytoplasmic and nuclear proteins were extracted using the protein extraction kit (cat. no. P0013B; Shanghai Beyotime Biological Science & Technology Co., Ltd.), and protein levels were then determined using a BCA protein assay kit (cat. no. P0010; Shanghai Beyotime Biological Science & Technology Co., Ltd.). Protein samples (30 µg) were run on a 10% SDS-PAGE gel, and then transferred to polyvinylidene fluoride membrane. Membranes were then blocked with 5% bovine serum albumin (cat. no. W029; Shanghai Bogu Biotechnology Co., Ltd., Shanghai, China) blocking solution for 2 h at room temperature, and then incubated overnight at 4°C with the following primary antibodies: Rabbit monoclonal antibody OCT4 (1:1,000; cat. no. ab200834), rabbit monoclonal antibody CD44 (1:1,000; cat. no. ab51037), mouse monoclonal antibody CD24 (1:1,000; cat. no. ab76514), rabbit monoclonal antibody CD133 (1:1,000; cat. no. ab216323), rabbit monoclonal antibody SOX2 (1:1,000; cat. no. 3579) and mouse monoclonal antibody ABCG2 (1:1,000; cat. no. ab130244). Following overnight incubation, the membranes were washed three times with Tris-buffered saline with 0.1% Tween-20 (TBST), and goat anti-mouse IgG (1:1,000; cat. no. ab205719) and goat anti-rabbit IgG (1:1,000; cat. no. ab205718) were incubated at 37°C for 2 h. The membrane was then washed three times with TBST, and then visualized using enhanced chemiluminescent reagents (cat. no. P0018; Shanghai Beyotime Biological Science & Technology Co., Ltd.) according to the previously published protocol (19). ImageJ software (version 1.48; National Institutes of Health, Bethesda, MD, USA) was used for densitometric analysis of target protein bands. Experiments were performed in triplicate.

Establishment of the xenograft nude mouse model. Spheroid cells generated from LoVo and HCT-116 cells were labeled as LoVocsc and HCT-116csc, respectively. LoVo, LoVocsc,

HCT-116 and HCT-116csc cells were harvested, rinsed twice with ice-cold PBS and then re-suspended with normal saline in order to obtain cell suspensions with a concentration of 2×10^6 cells/ml, which were then placed on ice for subsequent injections. A total of 0.2 ml of cell suspension of LoVo, LoVocsc, HCT-116 and HCT-116csc groups were injected subcutaneously into the right fossa axillaris of 12 randomly selected nude mice (each cell suspension group injected into 3 nude mice). When the xenografts had grown to ~ 0.8 -1.5 cm, the mice were sacrificed and the tumors were isolated. The tumor tissue was then dissected into 1 mm³ blocks and inoculated subcutaneously into the right fossa axillaris of nude mice under sterile conditions. Tumors formed from LoVo and HCT-116 cells were subsequently inoculated into 24 nude mice (12 mice per tumor type). Tumors formed from LoVocsc and HCT-116csc cells were inoculated into 64 nude mice (32 mice per tumor type). Every 2 days, major and minor axes of the tumors were measured using a vernier caliper, denoted as a and b, respectively; to determine the tumor volumes (V) using the following formula:

$$V (\text{mm}^3) = 1 / 2 * a * b^2 \quad (20)$$

When xenografts had grown to a size of 100 mm³, 8 nude mice bearing LoVo, HCT-116, LoVocsc and HCT-116csc xenografts were randomly selected (2 mice per tumor type). These mice were sacrificed via cervical dislocation, and the tumor tissues were obtained for subsequent experimentation.

H&E staining. Tissues were collected, fixed with 4% paraformaldehyde for 10 min at room temperature, paraffin-embedded and sectioned (5 μm thick sections). Following dewaxing with xylene and rehydrated using a descending ethanol series for 2 min per concentration gradient (100, 90, 80 and 70%), sections were stained using a H&E staining kit (cat. no. C0105; Shanghai Beyotime Biological Science & Technology Co., Ltd.), in accordance with the manufacturer's protocol, and subsequently dehydrated with gradient ethanol for 10 sec per concentration gradient (70, 80, 90 and 100%). Sections were then mounted and histopathological changes were observed under a light microscope (magnification, x100 and x400) (21).

Grouping and SalB dosing. The remaining mice bearing LoVocsc xenografts were randomly assigned into 6 groups (5 mice per group): LoVocsc group, LoVocsc + L-OHP group, LoVocsc + SalB-low dose (L) group, LoVocsc + SalB-medium dose (M) group, LoVocsc + SalB-high dose (H) group and LoVocsc + L-OHP + SalB-L group. The remaining mice bearing LoVo xenografts were randomly assigned into 2 groups (5 mice per group): LoVo group and LoVo + L-OHP group. The mice bearing HCT-116csc and HCT-116 xenografts were grouped using the aforementioned protocol. Mice in the LoVocsc + L-OHP and LoVo + L-OHP groups were intraperitoneally injected with L-OHP (0.5 mg); Mice in the LoVocsc + SalB-L, LoVocsc + SalB-M and LoVocsc + SalB-H groups were intragastrically administered low, medium and high doses of SalB solution (0.36, 0.72 and 1.44 g, respectively), at a dosage of 0.4 ml; Mice in the LoVocsc + L-OHP + SalB-L group were intraperitoneally injected with L-OHP (0.5 mg) combined with intragastric administration of low dose of SalB (0.36 g). Similarly, mice in the HCT-116csc + 5-FU and HCT-116 + 5-FU groups were intraperitoneally injected with 5-FU (0.01 mg); and

mice in the HCT-116csc + SalB-L, HCT-116csc + SalB-M and HCT-116csc + SalB-H groups were intragastrically administered low, medium and high doses of SalB solution (0.36, 0.72 and 1.44 g, respectively), at a dosage of 0.4 ml. Furthermore, the mice in the HCT-116csc + 5-FU + SalB-L group were intraperitoneally injected with 5-FU (0.01 mg) combined with intragastric administration of low dose of SalB (0.36 g). Mice in the LoVo, LoVocsc, HCT-116 and HCT-116csc groups were intragastrically administered 0.4 ml of normal saline. L-OHP and 5-FU were administered to respective groups once every two days, whereas SalB was administered every day. Treatment lasted for a total duration of 28 days. The activity and skin color of nude mice were recorded every day for 28 days and were then euthanized by cervical dislocation when they reached the pre-determined measureable end points: Weight loss exceeding 15%.

Determination of tumor volume, growth curves and the rate of tumor inhibition. At 3 day time intervals, major and minor axes of the tumors were determined using a vernier caliper to calculate the tumor volume. Using these data, growth curves of the tumors were determined. Furthermore, the inhibitory rate was determined using the following formula: Inhibitory rate = (mean tumor volume of the control group - mean tumor volume of the test group) / mean tumor volume of the control group * 100%. To investigate the interaction between SalB with L-OHP and 5-FU chemotherapeutic agents, the method described by Jin *et al.* (22) was used. This method provides a 'Q' value, according to which the interaction between two drugs can be classified as exhibiting an antagonistic effect ($Q \leq 0.85$), additive effect ($0.85 \leq Q < 1.15$) or synergistic effect ($Q \geq 1.15$). The formula used to calculate the Q value is as follows: $Q = E_{a+b} / (E_a + E_b - E_a * E_b)$, where E_{a+b} represents the mean effect of combination treatment, and E_a and E_b represent the effect of drug A and drug B alone, respectively.

Tumor CD44, CD133, SOX2 and ABCG2 expression levels determined by western blot analysis. Tumor tissues were lysed in radioimmunoprecipitation assay buffer (1 mg tumor tissue for 10 μl lysis buffer; cat. no. P0013B; Shanghai Beyotime Biological Science & Technology Co., Ltd.), and liquid nitrogen was quickly added to grind the tissues to extract protein. This was followed by centrifugation at 10,000 x g for 5 min at 4°C, and the supernatant was collected. Procedures for western blot were performed according to the aforementioned protocol. β -actin was used as an interval control.

Statistical analysis. Statistical analyses were performed using SPSS software (v. 18.0; SPSS, Inc., Chicago, IL, USA). Data are presented as mean \pm standard deviation for at least three separate experiments. Comparisons between two groups were performed using a Student's t-test, and multiple comparisons between groups was performed using one-way analysis of variance followed by the Newman-Keuls post hoc test. $P < 0.05$ was considered to indicate a statistically significant difference.

Results

Growth of spheroid CSCs. Human colon cancer cell lines LoVo and HCT-116 were cultured for 2 days (Fig. 1A and B) and then cultured in stem cell culture medium ES. Following

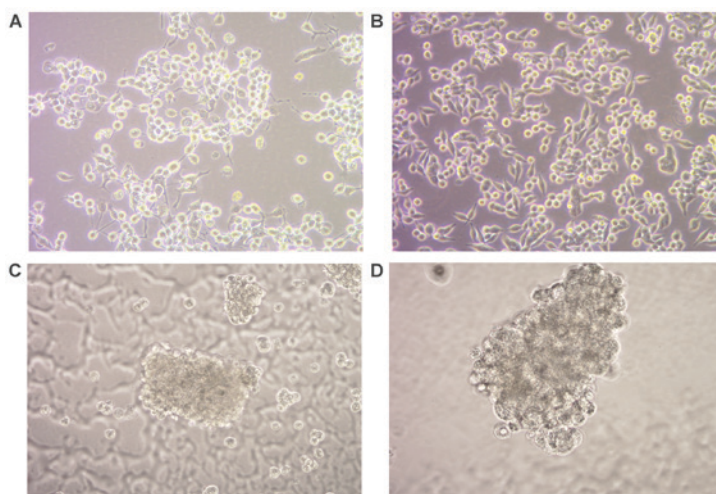


Figure 1. Observation of colon cancer cells using a light microscope. Human colon cancer cell lines (A) LoVo and (B) HCT-116 were observed after 2 days of culture. (C) LoVocsc and (D) HCT-116csc cells were observed following 5 days of culture (magnification, x200). cscs, cancer stem cells.

suspension culture for 2-3 days, only a small portion of cells survived. At the day 4 time interval, a small number of floating cell spheroids were visible, with a number of cells closely clustered. These cell spheroids were oval shaped and exhibited a clustered appearance, with a clear intercellular space (data not shown). The spheroids increased in size in a time-dependent manner and at days 5-6 time interval, suspended regular stem cell spheroids were visible and an increased number of cells, blurred intercellular space and strong refractivity was observed using a light microscope (Fig. 1C and D). Necrosis was observed in the center of the spheroids at the >10 day time intervals (data not shown). Spheroids were collected on days 5 and 6 for further experimentation.

Verifying CSC formation. FCM was performed to determine the expression of cell surface marker CD133 in populations of adherent and spheroid primary colon cancer cell populations. CD133 has been previously used as a marker for stem cells and to isolate colon CSCs from spheroids (23,24). The results demonstrated that there were significant differences in CD133 expression levels between the adherent LoVo ($1.48\pm 0.30\%$) and LoVocsc spheroid cells ($87.44\pm 4.32\%$; $P<0.01$; Fig. 2A). The levels of CD133⁺ cells in the adherent HCT-116 cells ($1.25\pm 0.24\%$) was also significantly decreased compared with HCT-116csc spheroid cells ($92.53\pm 3.56\%$; $P<0.01$; Fig. 2A).

RT-qPCR and western blot analyses were performed to determine the expression levels of the following stem cell markers in the parental and CSCs: CD24, CD44, CD90, SOX2, ABCG2, OCT4 and Nanog. As revealed in Fig. 2B, mRNA expression levels of CD24, CD44, CD133, SOX2 and ABCG2 were significantly increased in LoVocsc cells compared with LoVo cells ($P<0.01$; Fig. 2B). In addition, the protein expression levels of CD44, CD133, SOX2 and ABCG2 were significantly increased in LoVocsc cells compared with LoVo cells ($P<0.01$; Fig. 2B); whereas the expression of CD24 did not exhibit a significant difference (Fig. 2B). Furthermore, mRNA expression levels of OCT4, CD44, CD133, SOX2 and ABCG2 were significantly increased in HCT-116csc cells compared with HCT-116 cells ($P<0.01$; Fig. 2C), and their protein expression levels were

also significantly higher in HCT-116csc cells compared with HCT-116 cells, with the exception of OCT4 ($P<0.01$; Fig. 2C).

Histopathology of xenografts. 10-15 days following the subcutaneous injection of LoVo and HCT-116 cells, grain-like bulges in the right axillary appeared. By contrast, LoVocsc and HCT-116csc cells exhibited decreased oncogenic time, grain-like bulges appeared ~6-8 days post-injection (data not shown). When the xenografts grew to ~0.8-1.5 cm (measured at the major axis of the tumor), whole tumors were harvested, cut into sections and transplanted into the right armpit of the remaining nude mice. Soft, grain-like solid bulges were visible 4-5 days post-transplant, and the xenografts grew to a size of 100 mm³ 2 weeks post-injection (data not shown). No nude mice died during the modeling.

The results of HE staining revealed glandular cavities in the xenografts of the LoVo and HCT-116 group, whereas irregular growth was observed in the LoVocsc and HCT-116csc groups. In addition, large areas of necrotic tissue were observed in the core regions of the tumors in the LoVocsc and HCT-116csc groups. Compared with the LoVo and HCT-116 groups, xenografts of the corresponding LoVocsc and HCT-116csc groups exhibited an increased level of irregular structures, a decreased level of differentiation, a marked increase in nuclear atypia and an increased level of mitosis (Fig. 3), all of which indicated a higher malignancy in the tumors in the LoVocsc and HCT-116csc groups.

Treatment with L-OHP and 5-FU inhibits rate of tumor growth. No mice died during drug administration. Nude mice in the LoVocsc + L-OHP, HCT-116csc and HCT-116csc+5-FU groups gradually lost weight, with the HCT-116csc+5-FU group exhibiting the greatest weight loss. Furthermore, these groups exhibited lower activity as well as skin color deterioration; however, these conditions were not observed in the other groups (data not shown). Some of the mice suffered from ulcerations on the tumor surface when reaching the end of drug intervention. Such mice did not exhibit clinical evidence of pain or distress. In addition, the depth and size of the ulcer is very limited and did not exhibit any manifestation of infection

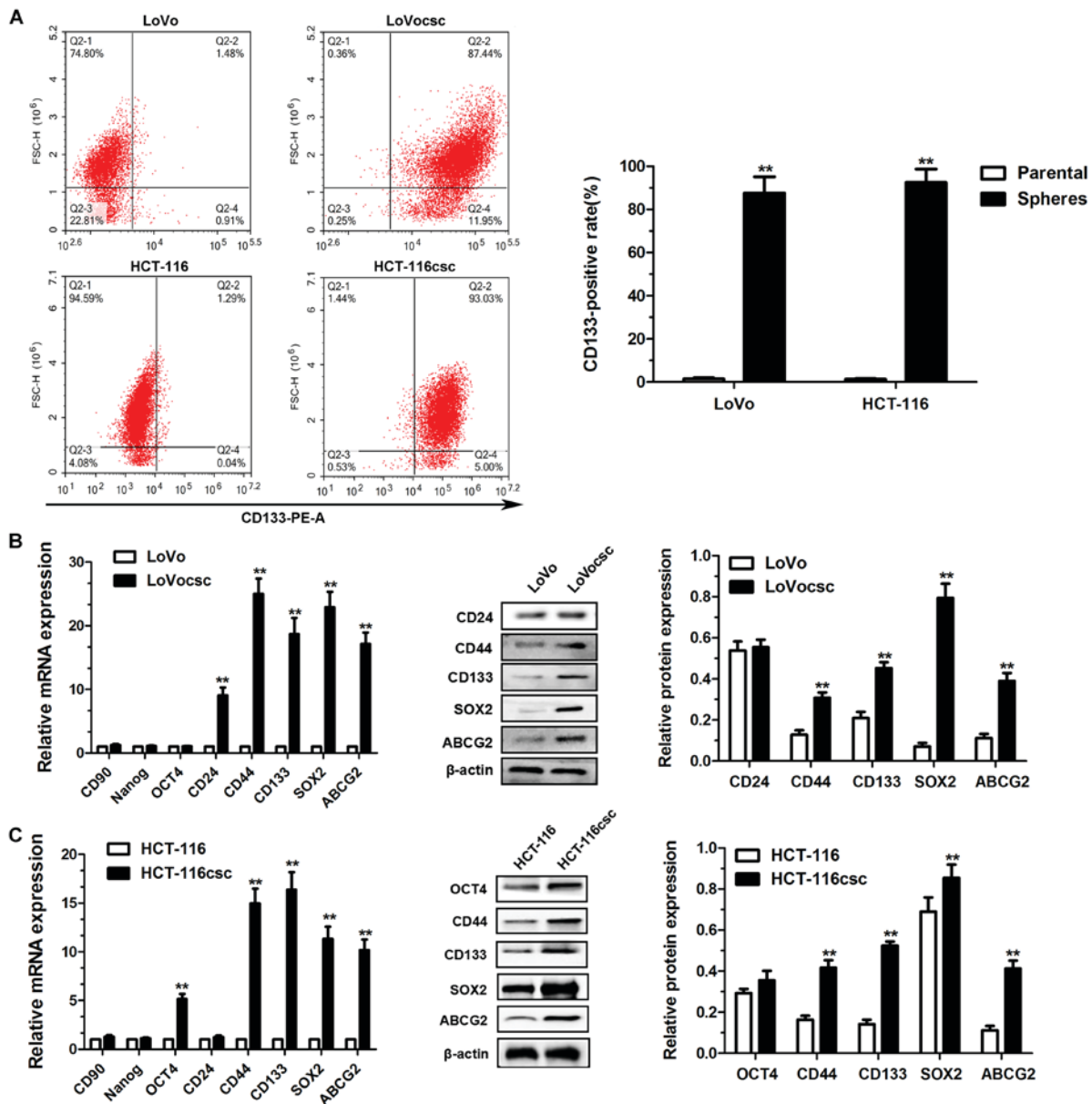


Figure 2. Identification of colon CSCs. (A) Flow cytometry analysis and quantification of CD133 expression in spheroid cells and corresponding parental cells. Cells in Q2-2 correspond to CD133-positive cells. Results are representative images of three independent experiments. **P<0.01 vs. parental cells. (B) Relative expression of stem cell markers at mRNA and protein levels in LoVo and LoVocsc cells. **P<0.01 vs. LoVo cells. (C) Relative expression of stem cell markers at mRNA and protein levels in HCT-116 and HCT-116csc cells. **P<0.01 vs. HCT-116 cells. Data are presented as mean \pm standard deviation. CSC, cancer stem cell; CD, cluster of differentiation; SOX2, transcription factor sox-2; ABCG2, ATP-binding cassette sub-family G member 2.

or hemorrhage, and so no clinical intervention regarding ulceration was performed. Mice belonging to the LoVocsc and HCT-116csc groups demonstrated a reduced oncogenic time (data not shown), and the growth rates of the tumors were markedly increased compared with their corresponding parental cells. Treatment with L-OHP was revealed to induce an inhibitory effect on tumor volumes in the LoVo and LoVocsc groups, where its inhibitory rate in the LoVo group was 44.98%, which was markedly higher compared with that exhibited by the LoVocsc group (33.92%; Fig. 4A and Table II). Treatment with 5-FU was also demonstrated to induce an inhibitory effect on tumor volume in HCT-116 and HCT-116csc groups compared with non-treated HCT-116 and HCT-116csc groups, which demonstrated inhibitory rates of 43.92 and 22.18%, respectively (Fig. 4B and Table III). These results suggested

that xenografts of the LoVocsc and HCT-116csc groups exhibited drug resistance, thus suggesting that the model was successfully established.

SalB attenuates drug resistance exhibited by colon CSCs xenografts. Prior to drug administration, tumor size was not significantly different between the different groups (P>0.05; Fig. 5 and Table IV). Following L-OHP and SalB administration, tumor volumes exhibited by the LoVocsc + L-OHP and LoVocsc + L-OHP + SalB-L groups were significantly reduced and demonstrated statistically significant differences compared with the LoVocsc group (P<0.01; Fig. 5A and Table IV). However, the LoVocsc + SalB-L group and the LoVocsc group did not demonstrate a significant difference in tumor volume post-drug administration

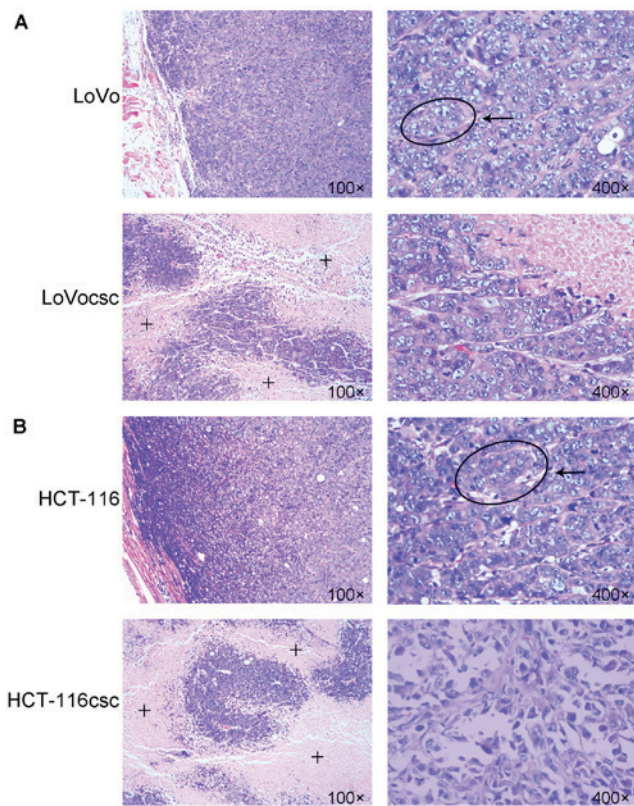


Figure 3. Pathological morphology of tumor tissues was investigated via H&E staining of (A) LoVo and LoVocsc cells and (B) HCT-116 and HCT-116csc cells. Cells undergoing necrosis are indicated by a '+' symbol; and glandular cavities are indicated using arrows (magnification, 100 and x400).

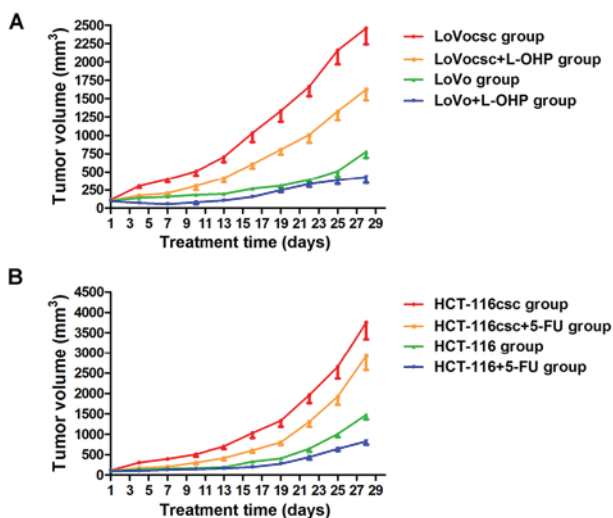


Figure 4. Chemotherapeutic agents were revealed to induce an inhibitory effect on xenografts. (A) Tumor growth curves for Balb/c nude mice in the LoVo and LoVocsc groups following administration of L-OHP. (B) Tumor growth curves for Balb/c nude mice in HCT-116 and HCT-116csc groups following administration of 5-FU. n=5. Data are presented as mean \pm standard deviation. csc, cancer stem cells; 5-FU, fluorouracil; L-OHP, oxaliplatin.

($P > 0.05$; Fig. 5A and Table IV). In addition, the tumor volume of the LoVocsc + L-OHP + SalB-L group was revealed to be suppressed compared with that exhibited by the LoVocsc + L-OHP group ($P < 0.01$; Fig. 5A and Table IV). Based on a previously described method by Jin *et al* (22), the Q

value was revealed to be 1.68 (data not shown), thus suggesting that SalB and L-OHP may exhibit a synergistic effect on the suppression of tumor volume, and that treatment with SalB may significantly reverse the drug resistance exhibited by LoVocsc xenografts in nude mice (Fig. 5A and Table IV). Furthermore, the results demonstrated that the tumor volumes of the LoVocsc + SalB-M and LoVocsc + SalB-H groups were $1,638.22 \pm 130.41$ and $1,270.15 \pm 108.58$ mm³, respectively; which were significantly smaller than that of the LoVocsc group ($2,456.69 \pm 216.35$ mm³) and LoVocsc + SalB-L group ($2,293.45 \pm 203.64$) ($P < 0.01$, data not shown). These results suggested that medium and high doses of SalB suppressed tumor volume in LoVocsc xenografts in a dose-dependent manner, whereas low doses of SalB did not exhibit marked antitumor activity.

Following 5-FU and SalB administration, tumor volumes exhibited by the HCT-116csc + SalB-L, HCT-116csc + 5-FU and HCT-116csc + 5-FU + SalB-L groups demonstrated statistically significant differences compared with that exhibited by the HCT-116csc group ($P < 0.05$ and $P < 0.01$; Table V). In addition, the tumor volume of the HCT-116csc + 5-FU + SalB-L group was revealed to be suppressed compared with that exhibited by the HCT-116csc + 5-FU group ($P < 0.01$; Fig. 5B and Table V). A Q value of 1.75 suggested that SalB and 5-FU may exhibit a synergistic effect on the suppression of tumor volume, and that treatment with SalB may significantly reverse the drug resistance exhibited by HCT-116csc xenografts in nude mice (Fig. 5B and Table V). Tumor volumes exhibited by the HCT-116csc, HCT-116csc + SalB-L, HCT-116csc + SalB-M and HCT-116csc + SalB-H groups were $3,756.20 \pm 416.92$, $3,289.15 \pm 383.58$, $2,857.24 \pm 255.62$ and $2,564.73 \pm 241.08$ mm³ respectively, indicating that SalB suppressed tumor volume in HCT-116csc xenografts in a dose-dependent manner ($P < 0.01$, data not shown).

SalB was revealed to attenuate drug resistance exhibited by colon CSCs xenografts in nude mice, thereby increasing tumor sensitivity to chemotherapeutic agents. In addition, SalB was revealed to inhibit tumor growth in a dose-dependent manner.

CD44, *CD133*, *SOX2* and *ABCG2* protein expression is regulated by SalB. Western blot analyses were used to determine the protein expression of stem cell markers CD44, CD133 and SOX2, as well as the drug resistance marker ABCG2, in all experimental groups. The results revealed that protein expression levels of CD44, CD133, SOX2 and ABCG2 exhibited by the LoVocsc and HCT-116csc groups were significantly increased compared with those exhibited by the LoVo and HCT-116 groups (Fig. 6A and B; $P < 0.01$). Protein expression levels of these four markers exhibited by the LoVocsc + SalB-L group were significantly decreased compared with the LoVocsc group ($P < 0.01$; Fig. 6A); whereas the expression levels of only three of these markers (CD44, SOX2 and ABCG2) were revealed to be significantly decreased in the HCT-116csc + SalB-L group compared with those exhibited by the HCT-116csc group ($P < 0.01$; Fig. 6B). These results demonstrate that low doses of SalB may significantly suppress CD44, SOX2 and ABCG2 protein expression in colon CSCs xenografts, which may contribute to the attenuation or reversal of drug resistance.

In addition, treatment with SalB was revealed to have an inhibitory effect on the protein expression levels of

Table II. Inhibitory rate of L-OHP on LoVo and LoVocsc xenografts (n=5).

Group	n	Tumor volume (mm ³)		Tumor inhibition rate (%)
		Pre-treatment	Post-administration	
LoVo	5	99.06±5.09	776.42±82.72	/
LoVo + L-OHP	5	96.07±7.20	427.19±78.33	44.98
LoVocsc	5	112.69±13.89	2,456.82±216.35	/
LoVocsc + L-OHP	5	106.07±17.10	1,623.58±147.86	33.92

L-OHP, oxaliplatin; csc, cancer stem cells; n, number of nude mice.

Table III. Inhibitory rate of 5-FU on HCT-116 and HCT-116csc xenografts (n=5).

Group	n	Tumor volume (mm ³)		Tumor inhibition rate (%)
		Pre-treatment	Post-administration	
HCT-116	5	117.42±11.37	1,476.38±112.07	/
HCT-116 + 5-FU	5	114.83±9.70	827.95±78.24	43.92
HCT-116csc	5	108.54±10.62	3,756.20±416.92	/
HCT-116csc + 5-FU	5	110.69±9.06	2,923.17±347.33	22.18

L-OHP, oxaliplatin; csc, cancer stem cells; n, number of nude mice; 5-FU, fluorouracil.

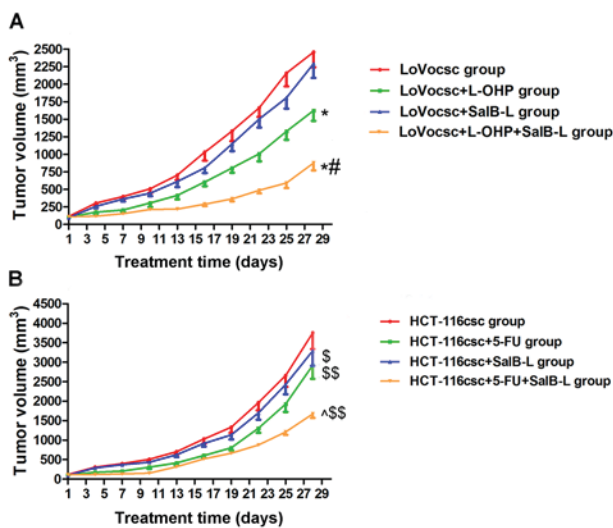


Figure 5. Effect of SalB on drug resistance in xenografts. (A) Tumor growth curves in the LoVocsc, LoVocsc + L-OHP, LoVocsc + SalB-L and LoVocsc + L-OHP + SalB-L groups. (B) Tumor growth curves in the HCT-116csc, HCT-116csc + 5-FU, HCT-116csc + SalB-L and HCT-116csc + 5-FU + SalB-L groups. Data are presented as mean ± standard deviation (n=5). *P<0.01 vs. LoVocsc group; #P<0.01 vs. LoVocsc + L-OHP group; \$P<0.05 and \$\$P<0.01 vs. HCT-116csc group; ^P<0.01 vs. HCT-116csc + 5-FU group. csc, cancer stem cells; 5-FU, 5-fluorouracil; L-OHP, oxaliplatin; SalB-L, low dose of salvianolic acid B.

CD44, SOX2 and ABCG2 in the LoVocsc xenografts in a dose-dependent manner (Fig. 6C; P<0.05 and P<0.01). As presented in Fig. 6C, protein expression levels of these three markers in the LoVocsc + SalB-L, LoVocsc + SalB-M and LoVocsc + SalB-H groups were significantly decreased

in a dose-dependent manner and exhibited a statistically significant difference compared with associated expression levels exhibited by the LoVocsc group (Fig. 6C; P<0.05 and P<0.01). CD133 expression levels did not demonstrate a significant difference between the LoVocsc + SalB-M and LoVocsc + SalB-H groups (Fig. 6C; P>0.05); however, it was significantly decreased compared with the expression levels exhibited by the LoVocsc and LoVocsc + SalB-L groups (Fig. 6C; P<0.01). Furthermore, there were no significant differences in the expression levels of CD44, CD133, SOX2 and ABCG2 proteins exhibited by the HCT-116csc + SalB-L, HCT-116csc + SalB-M and HCT-116csc + SalB-H groups; however, the expression levels of CD44, SOX2 and ABCG2 were significantly suppressed compared with the HCT-116csc group (Fig. 6D; P<0.05).

Discussion

Cancer MDR refers to the phenomenon that tumor cells are resistant to the effects of numerous antineoplastic drugs, regardless of their chemical structure or target. MDR in tumors is a complex process and involves numerous mechanisms (25).

CSCs are specialized cell populations of cancer cells with unlimited potential to proliferate, self-renew and differentiate into numerous cell types (24). CSCs promote rapid proliferation of tumors, and can induce tumor differentiation into malignancies that are of greater maturity, both in function and phenotype (26). CSCs exhibit the primary characteristics of drug resistance, as they express high levels of ABC transporter families on their cell membrane, which tends to enhance the efflux of chemotherapeutic drugs, thus

Table IV. Inhibitory rate of tumor growth in the L-OHP, low doses of SalB, and L-OHP combined with low doses of SalB in xenografts obtained from the LoVocsc group (n=5).

Group	n	Tumor volume (mm ³)		Tumor inhibition rate (%)
		Pre-administration	Post-administration	
LoVocsc	5	112.69±13.89	2,456.82±216.35	/
LoVocsc + L-OHP	5	106.07±17.10	1,623.58±147.86 ^a	33.92
LoVocsc + SalB-L	5	95.14±7.58	2,293.45±203.64	6.65
LoVocsc + L-OHP + SalB-L	5	110.29±8.43	875.30±106.21 ^{a,b}	64.37

^aP<0.01 vs. LoVocsc group; ^bP<0.01 vs. LoVocsc + L-OHP group. L-OHP, oxaliplatin; csc, cancer stem cells; n, number of nude mice; SalB-L, low dose of salvianolic acid B.

Table V. Inhibitory rate of tumor growth following treatment with 5-FU, low doses of SalB, and 5-FU combined with low doses of SalB in xenografts obtained from the HCT-116csc group (n=5).

Group	n	Tumor volume (mm ³)		Tumor inhibition rate (%)
		Pre-administration	Post-administration	
HCT-116csc	5	108.54±10.62	3,756.20±416.92	/
HCT-116csc + 5-FU	5	110.69±9.06	2,923.17±347.33 ^b	22.18
HCT-116csc + SalB-L	5	107.33±10.14	3,289.15±383.58 ^a	12.43
HCT-116csc + 5-FU + SalB-L	5	110.86±9.15	1,667.37±106.81 ^{b,c}	55.61

^aP<0.05 and ^bP<0.01 vs. HCT-116csc group; ^cP<0.01 vs. HCT-116csc + 5-FU group. csc, cancer stem cells; n, number of nude mice; 5-FU, fluorouracil; SalB-L, low dose of salvianolic acid B.

resulting in greater resistance of cancer cells to cytotoxicity and apoptotic induction by a variety of chemotherapeutic agents (27,28). ABCG2 is an important member of the ABC transporter family that is directly involved in the induction of drug resistance; however, it also maintains the stem cell characteristics of cancer cells. Thus, ABCG2 may represent a marker for cancer stem cells in numerous cancer types (29,30). Deng *et al* (31) demonstrated that CSCs present in malignant fibrous fibrohistiocytoma expressing high levels of ABCG2 were able to self-renew and exhibited a strong resistance to doxorubicin and cisplatin. SOX is a transcription factor protein family characterized by a homologous sequence called the high mobility group-box. SOX2 is a member of the SOX protein family, and is an important stem cell marker for inducing stem cell formation, maintaining the characteristics of stem cells as well as inhibiting the differentiation of stem cells (32). The association between SOX2 and CSC resistance has been extensively demonstrated (33,34). In addition, CD44 is a transmembrane glycoprotein belonging to the adhesion molecule family and serves a role in numerous physiological and pathological processes. CD44 has been demonstrated to serve a significant role in tumor invasion, metastasis and drug resistance (35). Yan *et al* (36) and Bourguignon *et al* (37) have demonstrated that CD44 is closely associated with drug resistance exhibited by colon CSCs.

With the increasing interest and research regarding CSCs, colon CSCs have been successfully isolated from colon cancer

solid tumors, colon cancer ascites and colon cancer cell lines (38). Furthermore, a number of studies have revealed that colon CSCs are closely associated with primary and secondary multidrug resistance of colon cancer (39,40). Despite the existence of CSCs having been demonstrated in the 1970s, the gold standard for isolating CSCs, as well as the development of animal xenograft models, have not been fully established. LoVo and HCT-116 cells were selected for investigation in the present study for the two reasons: Firstly, cell lines are readily available as a pure population compared with cells from colon cancer metastases; Second, the cells exhibit stable biological characteristics; The results of the present study suggested that colon CSCs LoVocsc and HCT-116csc derived from LoVo and HCT-116 cells stably express stem cell-like characteristics and xenografts generated by subcutaneous inoculation of colon CSCs LoVocsc and HCT-116csc can be serially passaged in mice. In addition, the results of the present study demonstrated that xenograft tumors exhibited drug resistance, rapid proliferation and other malignant biological characteristics. During modeling and drug administration, none of the mice died, however, some did exhibit weight loss. This suggested that the technique used to isolate CSCs and the method used to establish the nude mouse model was effective.

The results of the present study revealed that the serum-free suspension culture method may be used to isolate colon CSCs from LoVo and HCT-116 adherent cells. Furthermore, it was revealed that the xenografts obtained by subcutaneous

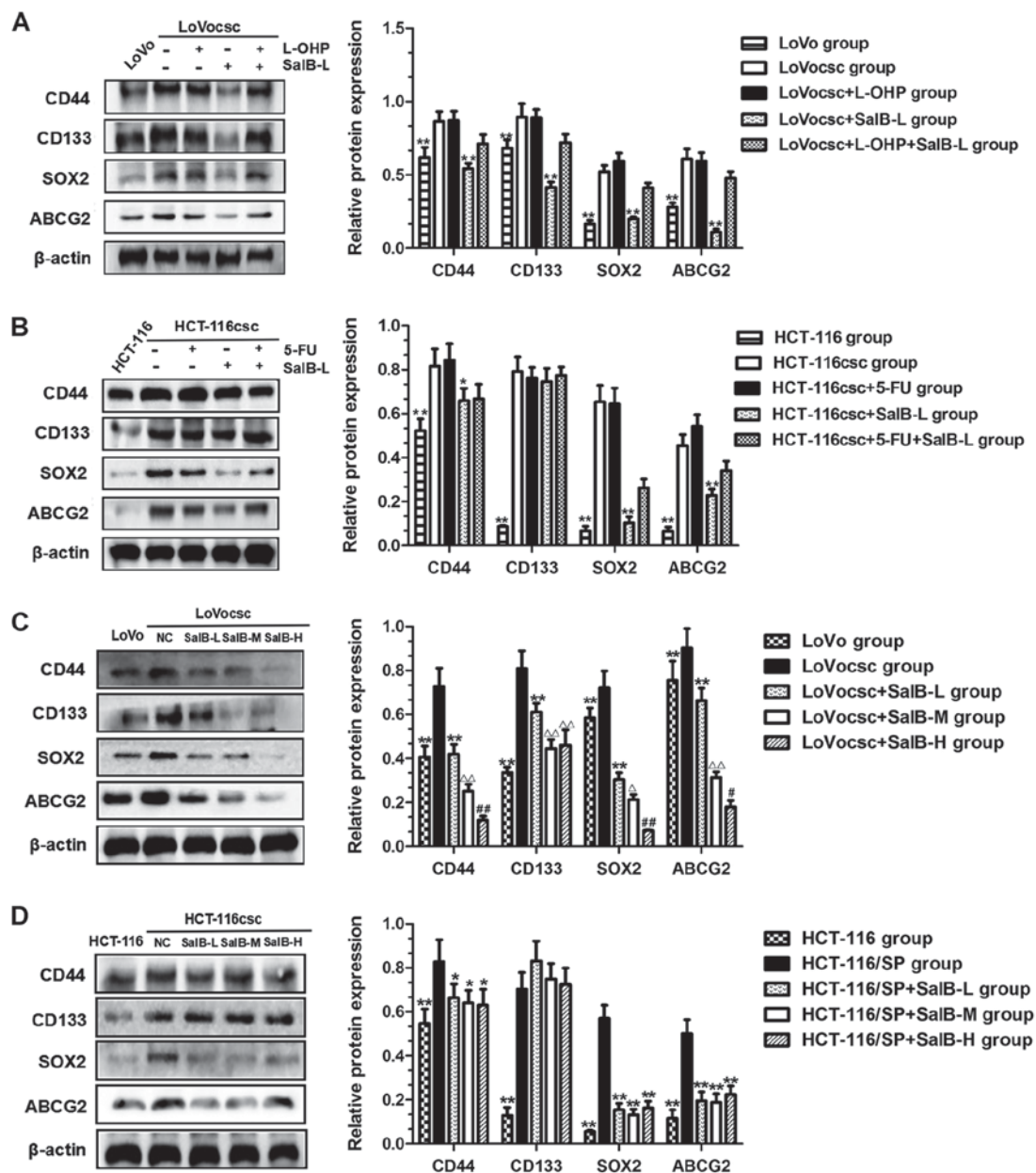


Figure 6. SalB regulates the expression of CD44, CD133, SOX2 and ABCG2 proteins. (A) Protein expression of CD44, CD133, SOX2 and ABCG2 in LoVo, LoVocsc, LoVocsc + L-OHP, LoVocsc + SalB-L and LoVocsc + L-OHP + SalB-L groups. (B) Protein expression of CD44, CD133, SOX2 and ABCG2 in HCT-116, HCT-116csc, HCT-116csc + 5-FU, HCT-116csc + SalB-L and HCT-116csc + 5-FU + SalB-L groups. (C) Protein expression of CD44, CD133, SOX2 and ABCG2 in LoVo, LoVocsc, LoVocsc + SalB-L, LoVocsc + SalB-M and LoVocsc + SalB-H groups. ^{**}P<0.01 vs. LoVocsc group; ^ΔP<0.05 and ^{ΔΔ}P<0.01 vs. LoVocsc + SalB-L group; [#]P<0.05 and ^{##}P<0.01 vs. LoVocsc + SalB-M group. (D) Protein expression of CD44, CD133, SOX2 and ABCG2 in HCT-116, HCT-116csc, HCT-116csc + SalB-L, HCT-116csc + SalB-M and HCT-116csc + SalB-H groups. ^{*}P<0.05 and ^{**}P<0.01 vs. HCT-116csc group. Data are presented as mean ± standard deviation. csc, cancer stem cells; 5-FU, fluorouracil; L-OHP, oxaliplatin; SalB, salvianolic acid B; -L, low dose; -M, medium dose; -H, high dose; NC, negative control; CD, cluster of differentiation; SOX2, transcription factor sox-2; ABCG2, ATP-binding cassette sub-family G member 2.

inoculation of LoVocsc and HCT-116csc cells could be serially passaged in mice. The growth rate of the tumors in the LoVocsc and HCT-116csc groups was demonstrated to be increased compared with rates exhibited by the LoVo and HCT-116 groups. Furthermore, the xenografts exhibited a high malignancy as determined by H&E staining and were resistant to chemotherapy drugs, such as L-OHP and 5-FU. In addition, the derived CSCs from the LoVocsc and HCT-116csc groups exhibited significantly increased expression levels of CD44, CD133, SOX2 and ABCG2 proteins compared with corresponding LoVo and HCT-116 groups. *In vivo* experiments

revealed that treatment with L-OHP or 5-FU combined with SalB had an inhibitory effect on tumor growth and demonstrated a greater efficacy compared with treatment with L-OHP or 5-FU alone. The determined Q values were >1.15, which, based on the method by Jin *et al* (22), suggested that SalB, when used in combination with L-OHP or 5-FU, exhibited a synergistic inhibition of tumor growth. This suggested that SalB could significantly attenuate the drug resistance of xenografts, and thus improve the efficacy of chemotherapeutic agents. Furthermore, the results of the present study demonstrated that SalB suppressed tumor growth in

a dose-dependent manner. In addition, western blot analysis revealed that treatment with SalB significantly decreased the expression levels of CD44, SOX2 and ABCG2 proteins in LoVocsc and HCT-116csc xenografts, and this was exhibited in a dose-dependent manner in LoVocsc xenografts.

In conclusion, the results of the present study revealed that serum-free suspension cultures may be used to effectively isolate colon CSCs from LoVo and HCT-116 cells. Nude mice models bearing LoVocsc and HCT-116csc cells were successfully established, and treatment with SalB was demonstrated to effectively attenuate MDR exhibited by of colon CSCs xenografts via the suppression of CD44, SOX2 and ABCG2 protein expression levels.

A limitation of the present study was the absence of non-cancerous cell line to be used as a control. Future studies should focus on the observation of dynamic alterations of xenograft growth in the orthotopic transplant tumor model of colon CSCs in mice using *in vivo* optical imaging, as well as tumor invasion and metastasis of liver, lung, brain and other organs. Such investigations would serve to deepen the understanding of *in vivo* SalB treatment as a novel therapeutic strategy for the treatment of MDR in colon CSCs. In addition, in future studies we will aim to further investigate the anti-MDR effect of SalB using *in vitro* models as well as determine the effect of SalB on morphological changes of colon CSCs, including the cell refractive index, the cell cycle, drug resistance, proliferation and apoptosis. Furthermore, we will aim to uncover the molecular mechanism underlying the anti-MDR effect of SalB.

Acknowledgements

The authors would like to thank Dr Wenjing Wang (Medical Department, Shandong Xiehe College, Shandong, China) and Dr Li Min (Department of Anorectal, JiaDing Traditional Chinese Medicine Hospital, Shanghai University of Traditional Chinese Medicine, Shanghai, China) for their technical assistance.

Funding

No funding was received.

Availability of data and materials

All data generated or analyzed during this study are included in this published article.

Authors' contributions

PG, YL, JW and WG contributed to the study design. PG, YL, JW, WG, XL, SW, LX and BW performed the experiments. XL, SW and BW analyzed data and contributed to the writing of the manuscript. All authors reviewed the manuscript.

Ethics approval and consent to participate

All animal experiments were performed according to the guidelines of the Chinese Experimental Animals Administration Legislation and were approved by the Ethics Committee for Animal Experiments of Shanghai University

of Traditional Chinese Medicine (Shanghai, China; reference no. SZY 201504023).

Consent for publication

Not applicable.

Competing interests

The authors declare that they have no competing interests.

References

- Vtorushin SV, Khristenko KY, Zavyalova MV, Perelmuter VM, Litviakov NV, Denisov EV, Dulesova AY and Cherdyntseva NV: The phenomenon of multi-drug resistance in the treatment of malignant tumors. *Exp Oncol* 36: 144-156, 2014.
- Di C and Zhao Y: Multiple drug resistance due to resistance to stem cells and stem cell treatment progress in cancer (Review). *Exp Ther Med* 9: 289-293, 2015.
- Takeishi S and Nakayama KI: To wake up cancer stem cells, or to let them sleep, that is the question. *Cancer Sci* 107: 875-881, 2016.
- Kanwar JR, Samarasinghe RM, Kamalapuram SK and Kanwar RK: Multimodal nanomedicine strategies for targeting cancer cells as well as cancer stem cell signalling mechanisms. *Mini Rev Med Chem* 17: 1688-1695, 2017.
- Greve B, Kelsch R, Spaniol K, Eich HT and Götte M: Flow cytometry in cancer stem cell analysis and separation. *Cytometry A* 81: 284-293, 2012.
- Jin F, Li HS, Zhao L, Wei YJ, Zhang H, Guo YJ, Pang R, Jiang XB and Zhao HY: Expression of anti-apoptotic and multi-drug resistance-associated protein genes in cancer stem cell isolated from T905 glioblastoma multiforme cell line. *Zhonghua Yi Xue Za Zhi* 88: 2312-2316, 2008.
- Asuthkar S, Stepanova V, Lebedeva T, Holterman AL, Estes N, Cines DB, Rao JS and Gondi CS: Multifunctional roles of urokinase plasminogen activator (uPA) in cancer stemness and chemoresistance of pancreatic cancer. *Mol Biol Cell* 24: 2620-2632, 2013.
- Yin T, Wei H, Gou S, Shi P, Yang Z, Zhao G and Wang C: Cancer stem-like cells enriched in Panc-1 spheres possess increased migration ability and resistance to gemcitabine. *Int J Mol Sci* 12: 1595-1604, 2011.
- Cabang AB, De Mukhopadhyay K, Meyers S, Morris J, Zimba PV and Wargovich MJ: Therapeutic effects of the euglenoid ichthyotoxin, euglenophycin, in colon cancer. *Oncotarget* 8: 104347-104358, 2017.
- Tang YC, Zhang Y, Zhou J, Zhi Q, Wu MY, Gong FR, Shen M, Liu L, Tao M, Shen B, *et al*: Ginsenoside Rg3 targets cancer stem cells and tumor angiogenesis to inhibit colorectal cancer progression *in vivo*. *Int J Oncol* 52: 127-138, 2018.
- Guo P, Wang S, Liang W, Wang W, Wang H, Zhao M and Liu X: Salvianolic acid B reverses multidrug resistance in HCT-8/VCR human colorectal cancer cells by increasing ROS levels. *Mol Med Rep* 15: 724-730, 2017.
- Wang M, Sun G, Wu P, Chen R, Yao F, Qin M, Luo Y, Sun H, Zhang Q, Dong X and Sun X: Salvianolic Acid B prevents arsenic trioxide-induced cardiotoxicity *in vivo* and enhances its anticancer activity *in vitro*. *Evid Based Complement Alternat Med* 2013: 759483, 2013.
- Zhao Y, Hao Y, Ji H, Fang Y, Guo Y, Sha W, Zhou Y, Pang X, Southerland WM, Califano JA and Gu X: Combination effects of salvianolic acid B with low-dose celecoxib on inhibition of head and neck squamous cell carcinoma growth *in vitro* and *in vivo*. *Cancer Prev Res (Phila)* 3: 787-796, 2010.
- Wang C, Xie J, Guo J, Manning HC, Gore JC and Guo N: Evaluation of CD44 and CD133 as cancer stem cell markers for colorectal cancer. *Oncol Rep* 28: 1301-1308, 2012.
- Jin Y, Jiang Z, Guan X, Chen Y, Tang Q, Wang G and Wang X: miR-450b-5p suppresses stemness and the development of chemoresistance by targeting SOX2 in colorectal cancer. *DNA Cell Biol* 35: 249-256, 2016.
- An Y and Ongkeko WM: ABCG2: The key to chemoresistance in cancer stem cells? *Expert Opin Drug Metab Toxicol* 5: 1529-1542, 2009.

17. Zhang W, Stoica G, Tasca SI, Kelly KA and Meiningner CJ: Modulation of tumor angiogenesis by stem cell factor. *Cancer Res* 60: 6757-6762, 2000.
18. Livak KJ and Schmittgen TD: Analysis of relative gene expression data using real-time quantitative PCR and the 2(-Delta Delta C(T)) method. *Methods* 25: 402-408, 2001.
19. Wang M, Chen DQ, Chen L, Liu D, Zhao H, Zhang ZH, Vaziri ND, Guo Y, Zhao YY and Cao G: Novel RAS inhibitors poricoic acid zg and poricoic acid ZH attenuate renal fibrosis via a Wnt/ β -catenin pathway and targeted phosphorylation of smad3 signaling. *J Agric Food Chem* 66: 1828-1842, 2018.
20. Wang Z, Li L and Wang Y: Effects of Per2 overexpression on growth inhibition and metastasis, and on MTA1, nm23-H1 and the autophagy-associated PI3K/PKB signaling pathway in nude mice xenograft models of ovarian cancer. *Mol Med Rep* 13: 4561-4568, 2016.
21. Wu X, Shou Q, Chen C, Cai H, Zhang J, Tang S, Cai B, Tang D and Cao G: An herbal formula attenuates collagen-induced arthritis via inhibition of JAK2-STAT3 signaling and regulation of Th17 cells in mice. *Oncotarget* 8: 44242-44254, 2017.
22. Jin ZJ: Addition in drug combination (author's transl). *Zhongguo Yao Li Xue Bao* 1: 70-76, 1980 (In Chinese).
23. Zhou JY, Chen M, Ma L, Wang X, Chen YG and Liu SL: Role of CD44(high)/CD133(high) HCT-116 cells in the tumorigenesis of colon cancer. *Oncotarget* 7: 7657-7666, 2016.
24. Dou J, Ni Y, He X, Wu D, Li M, Wu S, Zhang R, Guo M and Zhao F: Decreasing lncRNA HOTAIR expression inhibits human colorectal cancer stem cells. *Am J Transl Res* 8: 98-108, 2016.
25. Hasan S, Taha R and Omri HE: Current opinions on chemoresistance: An overview. *Bioinformation* 14: 80-85, 2018.
26. Okamoto K, Ninomiya I, Ohbatake Y, Hirose A, Tsukada T, Nakanuma S, Sakai S, Kinoshita J, Makino I, Nakamura K, *et al.*: Expression status of CD44 and CD133 as a prognostic marker in esophageal squamous cell carcinoma treated with neoadjuvant chemotherapy followed by radical esophagectomy. *Oncol Rep* 36: 3333-3342, 2016.
27. Wei L, Chen P, Chen Y, Shen A, Chen H, Lin W, Hong Z, Sferra TJ and Peng J: Pien Tze Huang suppresses the stem-like side population in colorectal cancer cells. *Mol Med Rep* 9: 261-266, 2014.
28. Jia M, Wei Z, Liu P and Zhao X: Silencing of ABCG2 by MicroRNA-3163 inhibits multidrug resistance in retinoblastoma cancer stem cells. *J Korean Med Sci* 31: 836-842, 2016.
29. Hu J, Li J, Yue X, Wang J, Liu J, Sun L and Kong D: Expression of the cancer stem cell markers ABCG2 and OCT-4 in right-sided colon cancer predicts recurrence and poor outcomes. *Oncotarget* 8: 28463-28470, 2017.
30. Yanamoto S, Yamada S, Takahashi H, Naruse T, Matsushita Y, Ikeda H, Shiraishi T, Seki S, Fujita S, Ikeda T, *et al.*: Expression of the cancer stem cell markers CD44v6 and ABCG2 in tongue cancer: Effect of neoadjuvant chemotherapy on local recurrence. *Int J Oncol* 44: 1153-1162, 2014.
31. Deng L, Li D, Gu W, Liu A and Cheng X: Formation of spherical cancer stem-like cell colonies with resistance to chemotherapy drugs in the human malignant fibrous histiocytoma NMFH-1 cell line. *Oncol Lett* 10: 3323-3331, 2015.
32. Lundberg IV, Edin S, Eklöf V, Öberg Å, Palmqvist R and Wikberg ML: SOX2 expression is associated with a cancer stem cell state and down-regulation of CDX2 in colorectal cancer. *BMC Cancer* 16: 471, 2016.
33. Chou MY, Hu FW, Yu CH and Yu CC: Sox2 expression involvement in the oncogenicity and radiochemoresistance of oral cancer stem cells. *Oral Oncol* 51: 31-39, 2015.
34. Carina V, Zito G, Pizzolanti G, Richiusa P, Criscimanna A, Rodolico V, Tomasello L, Pitrone M, Arancio W and Giordano C: Multiple pluripotent stem cell markers in human anaplastic thyroid cancer: The putative upstream role of SOX2. *Thyroid* 23: 829-837, 2013.
35. Hu B, Ma Y, Yang Y, Zhang L, Han H and Chen J: CD44 promotes cell proliferation in non-small cell lung cancer. *Oncol Lett* 15: 5627-5633, 2018.
36. Yan Y, Zuo X and Wei D: Concise review: Emerging role of CD44 in cancer stem cells: A promising biomarker and therapeutic target. *Stem Cells Transl Med* 4: 1033-1043, 2015.
37. Bourguignon LY, Shiina M and Li JJ: Hyaluronan-CD44 interaction promotes oncogenic signaling, microRNA functions, chemoresistance, and radiation resistance in cancer stem cells leading to tumor progression. *Adv Cancer Res* 123: 255-275, 2014.
38. O'Brien CA, Pollett A, Gallinger S and Dick JE: A human colon cancer cell capable of initiating tumour growth in immunodeficient mice. *Nature* 445: 106-110, 2007.
39. Kim MJ, Koo JE, Han GY, Kim B, Lee YS, Ahn C and Kim CW: DDual-blocking of PI3K and mTOR improves chemotherapeutic effects on SW620 human colorectal cancer stem cells by inducing differentiation. *J Korean Med Sci* 31: 360-370, 2016.
40. Wilson BJ, Schatton T, Frank MH and Frank NY: Colorectal cancer stem cells: Biology and therapeutic implications. *Curr Colorectal Cancer Rep* 7: 128-135, 2011.



This work is licensed under a Creative Commons Attribution-NonCommercial-NoDerivatives 4.0 International (CC BY-NC-ND 4.0) License.